

RESEARCH PAPER

Auxin polar transport is essential for the development of zygote and embryo in *Nicotiana tabacum* L. and correlated with ABP1 and PM H⁺-ATPase activities

Dan Chen, Yujun Ren, Yingtian Deng and Jie Zhao*

Key Laboratory of the Ministry of Education for Plant Developmental Biology, College of Life Sciences, Wuhan University, Wuhan 430072, China

* To whom correspondence should be addressed: E-mail: jzhao@whu.edu.cn

Received 9 December 2009; Revised 6 February 2010; Accepted 18 February 2010

Abstract

Auxin is an important plant growth regulator, and plays a key role in apical–basal axis formation and embryo differentiation, but the mechanism remains unclear. The level of indole-3-acetic acid (IAA) during zygote and embryo development of *Nicotiana tabacum* L. is investigated here using the techniques of GC-SIM-MS analysis, immunolocalization, and the GUS activity assay of *DR5::GUS* transgenic plants. The distribution of ABP1 and PM H⁺-ATPase was also detected by immunolocalization, and this is the first time that integral information has been obtained about their distribution in the zygote and in embryo development. The results showed an increase in IAA content in ovules and the polar distribution of IAA, ABP1, and PM H⁺-ATPase in the zygote and embryo, specifically in the top and basal parts of the embryo proper (EP) during proembryo development. For information about the regulation mechanism of auxin, an auxin transport inhibitor TIBA (2,3,5-triiodobenzoic acid) and exogenous IAA were, respectively, added to the medium for the culture of ovules at the zygote and early proembryo stages. Treatment with a suitable IAA concentration promoted zygote division and embryo differentiation, while TIBA treatment obviously suppressed these processes and caused the formation of abnormal embryos. The distribution patterns of IAA, ABP1, and PM H⁺-ATPase were also disturbed in the abnormal embryos. These results indicate that the polar distribution and transport of IAA begins at the zygote stage, and affects zygote division and embryo differentiation in tobacco. Moreover, ABP1 and PM H⁺-ATPase may play roles in zygote and embryo development and may also be involved in IAA signalling transduction.

Key words: ABP1, embryo differentiation, IAA, *Nicotiana tabacum*, PM H⁺-ATPase, zygote division.

Introduction

Embryo development is a crucial event during the life cycle of higher plants. One of the most important questions during this event is how a single zygote undergoes the series of precise cell division and differentiation to develop into a mature embryo. There are many studies indicating the involvement and role of auxin in this process (Liu *et al.*, 1993; Steinmann *et al.*, 1999; Friml *et al.*, 2003; Jenik and Barton, 2005). Auxin distribution and transportation were visualized in *Arabidopsis* embryos by using expression

analysis of auxin carrier gene *PINs* and the synthetic auxin-responsive promoter *DR5* (Steinmann *et al.*, 1999; Friml *et al.*, 2003; Jenik and Barton, 2005). The result showed that auxin flows upward and accumulates in the embryo proper (EP) of the early proembryo, and then it flows in different directions and accumulates in the hypophysis and cotyledon tips of the differentiated embryo. Mutation analysis of auxin-related genes in *Arabidopsis* demonstrates that auxin probably participates in apical–basal pattern formation. It

Abbreviations: ABP1, auxin binding protein 1; DAP, days after pollination; EDC, 1-ethyl-3-(3-dimethylaminopropyl)-carbodiimide hydrochloride; EP, embryo proper; GC-SIM-MS, gas chromatography-mass spectrometry-selected ion monitoring; IAA, indole-3-acetic acid; PM, plasma membrane; RT, room temperature; SABC, streptavidin and biotinylated horseradish peroxidase complex; TEM, transmission electron microscopy; TIBA, 2, 3, 5-triiodobenzoic acid.

© 2010 The Author(s).

This is an Open Access article distributed under the terms of the Creative Commons Attribution Non-Commercial License (<http://creativecommons.org/licenses/by-nc/2.5>), which permits unrestricted non-commercial use, distribution, and reproduction in any medium, provided the original work is properly cited.

was reported that both the gain-of-function mutant of *AUX/IAA* transcription factor *BDL* (*IAA12*) and the loss-of-function mutant of auxin response factor 5 (*ARF5*) fail to form hypocotyls and embryonic roots (Hardtke *et al.*, 1998; Hamann *et al.*, 2002). The quadruple mutant of *YUCCAs* flavin monooxygenases, which encode the key enzymes in auxin biosynthesis, also display similar defective phenotypes of lost hypocotyls and of embryonic root meristems (Cheng *et al.*, 2007).

These studies in *Arabidopsis* demonstrate the basis of our previous knowledge about the role of auxin in embryo pattern formation; but there are still many problems in the study of how auxin is involved in embryo development, such as the difficulty of isolating embryos which are inaccessible and tucked away inside the ovules, the complexity of the auxin signal transduction pathway, the difficulty of obtaining mutants, and the very limited information about the genetic background of other plants. Thus, most of the evidence about the roles of auxin in embryo development come from *in vitro*-culture systems except for the studies in *Arabidopsis*. These studies indicate that auxin and its polar transport inhibitors can affect the differentiation of zygotic embryos *in vivo* or somatic embryos *in vitro* (Liu *et al.*, 1993; Fischer and Neuhaus, 1996; Fischer *et al.*, 1997; Hadfi *et al.*, 1998; Fischer-Iglesias *et al.*, 2001; Basu *et al.*, 2002; Rober-Kleber *et al.*, 2003; Larsson *et al.*, 2008). The treatment with high concentrations of exogenous indole-3-acetic acid (IAA) or its transport inhibitors lead to the alteration of embryo shape in *Fucus distichus* (Basu *et al.*, 2002), wheat (Fischer and Neuhaus, 1996; Fischer *et al.*, 1997; Fischer-Iglesias *et al.*, 2001; Rober-Kleber *et al.*, 2003), *Brassica juncea* (Liu *et al.*, 1993; Hadfi *et al.*, 1998), and Norway spruce (Larsson *et al.*, 2008). Some of these aberrant embryos resembled the defects found in mutants of the auxin efflux carrier gene *PINI* (Liu *et al.*, 1993; Hadfi *et al.*, 1998).

Auxin is considered as a small signal molecule which is perceived by its receptor and then induces physiological and biochemical reactions in cells which lead to cell morphology and structure changes. Auxin binding protein 1 (ABP1) is believed to be an important candidate for auxin receptor, because of its high activity to bind auxin (Napier and Venis, 1992) and its ability to mediate auxin-induced cell division and elongation in a number of tissues in plants, such as maize coleoptiles (Steffens *et al.*, 2001), pea internodes (Yamagami *et al.*, 2004), *Arabidopsis* seedlings (Braun *et al.*, 2008), tobacco BY2 cells (David *et al.*, 2007), and leaf cells (Chen *et al.*, 2001a). Furthermore, it was found that ABP1 may be important for embryo development because its mutation leads to the lethal phenotype of embryos at the globular embryo stage (Chen *et al.*, 2001b). As the lethal phenotype of the *abp1* mutation prevents further studies about its function in embryos, little is known about the role of ABP1 in embryo development.

Plasma membrane (PM) H⁺-ATPase is an electrogenic proton pump which has a role in the control of various cell events such as cell elongation (Rober-Kleber *et al.*, 2003), stomatal closure (Merlot *et al.*, 2007), and the regulation of

intracellular pH (Rober-Kleber *et al.*, 2003). By using ATP as the energy source, PM H⁺-ATPase pumps H⁺ from cytoplasm to the cell exterior, thus forming an electrochemical gradient across the PM and constituting the driving force for nutrient and K⁺ uptake into the cells (Bouche-Pillon *et al.*, 1994; Sondergaard *et al.*, 2004). PM H⁺-ATPase is regarded as a downstream molecule of the auxin-dependent signal transduction pathway (Kim *et al.*, 2001; Rober-Kleber *et al.*, 2003; Sondergaard *et al.*, 2004; Christian *et al.*, 2006). Evidence has shown that the final target protein in auxin-induced cell acidification and elongation is the PM H⁺-ATPase, for auxin can improve the transcription and translation of PM H⁺-ATPase as well as the activity of this protein (Harper *et al.*, 1994; Frías *et al.*, 1996; Rober-Kleber *et al.*, 2003; Sondergaard *et al.*, 2004). The expression of PM H⁺-ATPase was enhanced by auxin and it was concentrated in the more acidic scutellum cell of wheat embryos. This suggests the participation of the PM H⁺-ATPase in auxin-related cell elongation of the embryo scutellum (Rober-Kleber *et al.*, 2003). However, the relationship of auxin and PM H⁺-ATPase in zygote and embryo development of dicotyledonous plants is still unknown.

In this study, the change in IAA level during the development of the tobacco zygote and embryo was analysed by means of GC-SIM-MS, zygote and embryo isolation, *in vitro* ovule culture, IAA immunolocalization, and the GUS histochemical assay of *DR5::GUS* transgenic plants. The expression patterns of ABP1 and the PM H⁺-ATPase in the zygote and embryo were also visualized for the first time using immunolocalization techniques, and the relationship between auxin, ABP1, and PM H⁺-ATPase in zygote and embryo development is also discussed.

Materials and methods

Plant materials

Nicotiana tabacum L. cv. SR1 and *DR5::GUS* transgenic plants (kindly provided by Professor Alice Cheung, University of Massachusetts, USA) were grown in a greenhouse at Wuhan University at 25–27 °C with a photoperiod of 16/8 h light/darkness. The flowers were artificially pollinated after anthesis in order to get embryos at the same developmental stages.

Quantification analysis of IAA by GC-SIM-MS

For IAA quantification analysis, 0.5 g fresh weight of tobacco ovules at different developmental stages (1, 3, 4, 6, 8, 10, and 15 d after pollination, DAP) were immediately frozen in liquid nitrogen. The extraction and purification of endogenous IAA was performed using the method described by Ding *et al.* (2008). The purified samples were methylated by a stream of diazomethane gas, resuspended in 100 µl of ethyl acetate, and analysed by gas chromatography-mass spectrometry-selected ion monitoring (GC-SIM-MS). The quantification protocol was conducted as described by Ribnichy *et al.* (2002) with some modifications. A Shimadzu GCMS-QP2010 Plus equipped with a HP-5MS column (30 m long, 0.25 mm i.d., 0.25 µm Film, Agilent, USA) was used to determine the level of IAA. The chromatographic parameters were as follows: injection temperature at 280 °C and initial oven temperature 70 °C for 1 min followed by a temperature programme of 160 °C to 240 °C. The standard IAA and D₂-IAA was from Sigma-Aldrich

(MO, USA). The monitored ions were *m/z* 130 and 132 (quinolinium ions from native IAA and D₂-IAA internal standard, respectively), and *m/z* 77, 189, and 191 (molecular ion and m⁺+6).

Isolation of zygotes and proembryos

The zygotes and two-celled proembryos of tobacco were isolated according to the methods reported previously by Qin and Zhao (2006). Firstly, ovules were dissected from ovaries at 3 DAP and 4 DAP and placed into an enzyme solution containing 13% mannitol, 3 mM 2-[*N*-morpholino] ethanesulphonic acid (MES), 3 mM polyvinylpyrrolidone K30 (PVP K30), 1% cellulose R-10, and 0.8% macerozyme R-10, pH 5.7, and then incubated with vibration for 30 min on an oscillator (ZW-A, FU-HUA). Secondly, ovules were washed three times at room temperature (RT) and the fertilized embryo sacs were released from the ovules by gently pressing with a small glass pestle. Thirdly, the embryo sacs were collected onto a slide using a micropipette and treated with an enzymatic solution containing 13% mannitol, 3 mM MES, 3 mM PVP K30, 0.25% cellulose R-10, and 0.2% macerozyme R-10, pH 5.7 for 2–5 min. The zygotes or two-celled proembryos were then isolated from the embryo sacs with self-made microneedles using an inverted microscope (Olympus CK30).

The isolation of tobacco multicellular embryos was performed as described by Zhang *et al.* (2008). Ovules at 5–12 DAP were treated with an enzymatic solution containing 8% mannitol, 3 mM MES, 3 mM PVP K30, 1% cellulose R-10, and 0.8% macerozyme R-10, pH 5.7 at 25 °C for 10–30 min. The embryos were isolated from treated ovules with microneedles, and collected using a micropipette under an inverted microscope (Olympus CK30).

Ovule culture

Ovaries at the zygote stage (3 DAP) and the early globular embryo stage (5 DAP) were sterilized in 70% ethanol for 0.5 min and in 2% NaClO for 4 min. After rinsing four times with sterile water, the ovules were isolated and cultured in MS medium (pH 5.8) supplemented with 6–8% sucrose, 0.25% phytigel, 0.1–4 μM IAA and different concentrations of 2, 3, 5-triiodobenzoic acid (TIBA; 10, 30 or 50 μM) at 25 °C in the dark. After 5 d and 10 d of culture, some ovules were fixed to observe embryo development inside the ovules. The others were transferred into fresh MS medium supplemented with 2% sucrose and 0.25% phytigel, pH 5.8 and cultured at 25 °C in the dark until maturity. They were then kept in 16/8 h light/dark to continue their development for 50 d. All experiments were repeated at least four times, the standard errors and *P*-values were calculated.

GUS histochemical assay

The *DR5* promoter comprises seven-copy tandem direct sequences that include the auxin-responsive element TGTCTC which is located upstream of a minimal 246 cauliflower mosaic virus 35S promoter (Ulmasov *et al.*, 1997). This promoter shows strong auxin responsiveness in plants (Tao *et al.*, 2002; Chen and Zhao, 2008). For GUS visualization in *DR5-GUS* transgenic tobacco, zygotes and proembryos were isolated from ovules without fixation and incubated in a reaction buffer with 50 mM NaPO₄ (pH 7.0), 0.1% (v/v) Triton X-100, 0.5 mM K₃[Fe(CN)₆], 0.5 mM K₄[Fe(CN)₆], 1.0 mg ml⁻¹ X-Gluc (Amresco Inc., USA) at 37 °C in darkness for 4–6 h. They were further cleared in a solution of 100% chloral hydrate:90% lactic acid (2:1, v/v) at room temperature (RT) for 30 min (Ren and Zhao, 2009), and then observed under a BH-2 microscope (Olympus, Japan) and photographed with a CoolSNAP digital camera system (RS Photometrics, USA).

For detecting *GUS* expression in ovules, ovules were kept in a solution containing 50 mM NaPO₄ (pH 7.0) and 100 mM DTT (DL-dithiothreitol), then transferred into the GUS staining solution containing 50 mM NaPO₄ (pH 7.0), 0.1% (v/v) Triton X-100, 5%β-mercaptoethanol, 1.0 mg ml⁻¹ X-Gluc (Amresco Inc., USA)

and covered with several drops of mineral oil. After being kept at 37 °C in darkness for 12 h, the ovules were directly observed under an Olympus SZX12 stereomicroscope and photographed with a CoolSNAP digital camera system (RS Photometrics, USA).

IAA immunoenzyme localization

Tobacco ovules were dissected from ovaries and immediately fixed in FPA solution (formaldehyde:propionic acid:70% ethanol, 5:5:90 by vol.) containing 2% (w/v) 1-ethyl-3-(3-dimethylaminopropyl)-carbodiimide hydrochloride (EDC; BioBasic Inc., Canada) overnight at 4 °C. The fixed ovules were rinsed and permeated with a decreasing series of ethanol solution (70, 50, 30, and 15%) and finally into water. The ovules were placed into an enzyme solution containing 2% cellulose R-10 and 1.5% macerozyme R-10 in 10 mM PBS (pH 7.2), incubated for 3 h at 30 °C, and then washed with 10 mM PBS. The embryos were isolated from the treated ovules with self-made microneedles using an inverted microscope (Olympus CK40, Japan). The SABC (streptavidin and biotinylated horseradish peroxidase complex) immunoenzyme method was used to detect IAA in the embryos. The experiments were performed as described by Zhang *et al.* (2008) with some modifications. The embryos were incubated in 3% H₂O₂ for 15 min, washed three times with distilled water for 5 min each time at RT. They were washed with a block solution (containing 5% BSA in 10 mM PBS, pH 7.2) for 20 min at RT, incubated with 1:300 dilutions (10 mM PBS, 1% BSA, pH 7.2) of IAA antibody overnight at 4 °C, rinsed three times with 10 mM PBS, and incubated with biotin-labelled goat anti-rat IgG antibody for 20 min at 37 °C. They were then rinsed three times with 10 mM PBS and treated with the SABC reagent for 20 min at 37 °C. After an extensive wash in 10 mM PBS supplemented with 0.02% (v/v) Tween-20 three times and in PBS twice, the embryos were stained with the AEC kit. The control samples were treated similarly except that the primary antibody was substituted with PBS/BSA solution. The samples were then washed in distilled water and immediately examined under a microscope (Olympus BH-2, Japan).

Western blot of ABP1 and PM H⁺-ATPase

Western blot was used to investigate whether the anti-maize ABP1 antibody (kindly provided by Professor Richard Napier, Crop Improvement and Biotechnology, Horticulture Research International, UK) could combine with ABP1 in tobacco. The total proteins from the mixed samples of 1, 3, 4, 6, 8, 10, and 15 DAP ovules were analysed by SDS-PAGE using a 15% acrylamide separating gel and a 5% acrylamide stacking gel in a Mini-Protean II electrophoresis cell (Bio-Rad). Equal amounts of the total proteins were loaded into each well. Gels were electroblotted (100 V, 1 h) onto nitrocellulose transfer membranes using an electrotransfer buffer (20 mM TRIS base, 150 mM glycine, and 20% methanol). The membranes were blocked with 5% non-fat dried milk in TBST buffer (20 mM TRIS base, 500 mM NaCl, and 0.05% Tween-20, pH 7.5) overnight at 4 °C. The membranes were then incubated with the primary ABP1 antibody (diluted 1:600) for 2 h at room temperature, and washed with TBST buffer for 3–10 min. They were incubated with alkaline-phosphatase-conjugated goat anti-rabbit antibody (1:500; Sino-American Biotechnology Co.) for 1 h, washed with TBST buffer three times, and then stained with nitro blue tetrazolium/5-bromo-4-chloro-3-indolyl phosphate (Sino-American Biotechnology Co.).

The specific binding activity of the anti-PM H⁺-ATPase antibody which comes from *N. plumbaginifolia* was also detected by Western blot. This antibody was generously provided by Professor Marc Boutry (Unité de Biochimie Physiologique, Institut des Sciences de la Vie, Université Catholique de Louvain-la-Neuve, Belgium) and has successfully been used to detect the expression of PM H⁺-ATPase in *N. plumbaginifolia* (Morsomme *et al.*, 1998), and pollen tubes of *Nicotiana plumbaginifolia* (Lefebvre *et al.*, 2005) and *Torenia fournieri* (Wu *et al.*, 2008). The procedure for

the PM H⁺-ATPase Western blot was similar to that of ABP1, except that the dilution of the primary antibody (Rabbit antibodies against *N. plumbaginifolia* H⁺-ATPase) is 1:500, and the secondary antibody is alkaline-phosphatase-conjugated goat anti-rabbit antibody (diluted 1:1000).

Immunoenzyme and immunofluorescence localization of ABP1 and PM H⁺-ATPase

For immunoenzyme localization, the ovules and embryos were isolated and fixed as described above. The embryos were rinsed with 4% sucrose in 10 mM PBS for 30 min, fixed in embedding medium, and frozen in liquid nitrogen. The embryo sections (12 μm thick) were cut longitudinally using a cryomicrotome (Leica Cryocut CM 3050S, Germany) and collected on slides coated with 0.01% poly-L-lysine. The immunoenzyme detection of ABP1 and PM H⁺-ATPase was performed using the SABC method. The sections were dried at 37 °C for 12 h before being incubated in 3% H₂O₂. The subsequent immunoprocurement was as previously described, the only difference being the type of antibodies utilized. The primary ABP1 and PM H⁺-ATPase antibodies were diluted to 1:100 with 10 mM PBS, and a biotin-labelled goat anti-rabbit IgG antibody were used as the secondary antibody.

For immunofluorescence localization, the isolated zygotes and embryos were rinsed three times with the PIPES buffer, once with 100 mM PBS, pH 7.4, and then incubated in the primary ABP1 and PM H⁺-ATPase antibodies diluted 1:50 with 100 mM PBS at 4 °C overnight. The samples were rinsed three times with 100 mM PBS, and then incubated with the secondary antibody, anti-rat-IgG-FITC conjugate (Sigma) diluted at 1:100 with 100 mM PBS for 1 h at 37 °C in the dark or at 4 °C overnight. The samples were rinsed three times with 100 mM PBS and examined under a microscope (Olympus, IMT-2). Control samples were incubated in 100 mM PBS instead of the primary antibody.

Immunogold localization of IAA, ABP1, and PM H⁺-ATPase

The early globular stage of embryos at 5 DAP were used. The method for IAA immunogold localization was the same as that described by Chen and Zhao (2008). The methods for ABP1 and PM H⁺-ATPase immunogold localization were similar to those described by Zhang *et al.* (2008), the only difference being the kind of antibodies used. The primary antibodies were ABP1 and PM H⁺-ATPase antibodies, respectively, and the secondary antibody was a goat anti-rabbit IgG antibody conjugated to 10 nm gold particles (Sigma). Ultrathin sections (about 60 nm) were cut using a Sorvall MT-6000 ultramicrotome and collected onto Formvar-coated nickel grids. After immunogold staining, the samples were examined and photographed under a transmission electron microscope (Hitachi H-800, Japan).

DAPI staining method

In order to observe zygote and early proembryo division clearly, all samples were stained with 2 μg ml⁻¹ DAPI for 10 min. The labelled blue fluorescence was then visualized and photographed under an inverted microscope (Olympus IMT-2, Japan).

Results

IAA level in ovules

By using the GC-SIM-MS technique, it was possible to detect the endogenous free IAA level in tobacco ovules (Fig. 1). Retention times of IAA/D₂-IAA were 9.753/9.736 min in the standard (Fig. 1A), and 9.758/9.739 min in the sample (Fig. 1B), respectively. The GC peaks of IAA and D₂-IAA obtained from the sample solutions were well separated

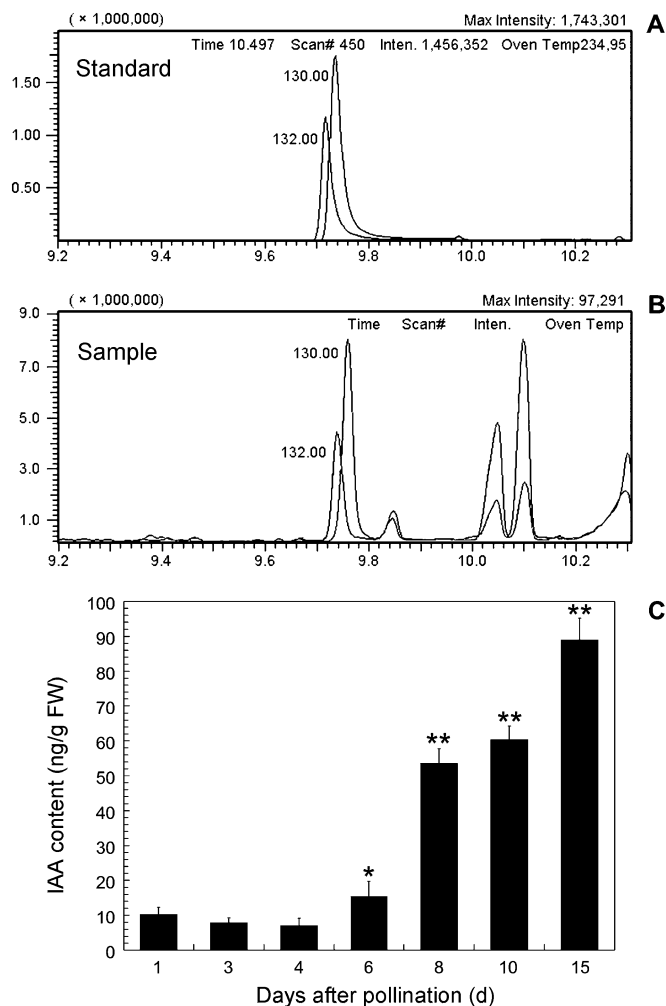


Fig. 1. Chromatograms (A, B) and contents (C) of IAA detected by GC-SIM-MS. (A) Retention times (RT) of IAA and D₂-IAA are 9.753 min and 9.736 min in the standards, respectively. (B) RT of IAA and D₂-IAA are 9.758 min and 9.739 min in the samples, respectively. Number 130.0 and 132.0 indicate the characteristic peak of IAA and D₂-IAA in (A) and (B), respectively. (C) Changes of IAA contents in tobacco ovules. The 1 DAP and 3 DAP ovules were at the egg and zygote stages, respectively. The ovules of 4, 6, 8, 10, and 15 DAP were at the stages of 2-celled, middle globular, heart-shaped, torpedo-shaped, and mature cotyledon embryos, respectively. IAA contents were measured in triplicate, and the standard error (s.e.) is shown. The number of ovaries for quantification analysis was 20–450 from 15 plantlets. * 0.01 < P < 0.05 indicates significant difference compared with the 3 DAP ovules at zygote stage; ** P < 0.01 indicates extremely significant difference compared with the 3 DAP ovules.

from the peaks of impurities (Fig. 1B). The changes in IAA level in ovules are shown in Fig. 1C. The IAA content was low in unfertilized (1 DAP) and fertilized ovules at the stages of the zygote (3 DAP) and the 2-celled embryo (4 DAP). It then increased 2-fold in the ovules (6 DAP) at the middle globular embryo stage when compared with the 3 DAP ovules, and significantly increased in the ovules at the heart-shaped embryo stage (8 DAP) and the torpedo-shaped

embryo stage (10 DAP). In the 15 DAP ovules at the mature cotyledon-embryo stage, the IAA level reached the maximum value of 89.02 ng g⁻¹ FW.

Distribution of IAA in isolated zygotes, embryos, and ovules in vivo

The distribution of free IAA in isolated zygotes and embryos of tobacco *DR5::GUS* transgenic plants was revealed by GUS staining (Fig. 2A–C, E–L). The GUS signal was weak, even in the elongated zygote and early proembryo stages (Fig. 2A–C). It then began to accumulate in the cells of the early globular embryo (Fig. 2E) and the IAA-dependent GUS signal gradually increased and displayed a polar distribution in the basal area of the embryo proper (EP) and in the whole suspensor of the middle globular embryo (Fig. 2F). When the cotyledon primordium

and provascular strands began to form, the GUS signal also appeared in these regions (Fig. 2G–J). The signals were obviously enhanced and distributed in the whole torpedo-shaped and mature cotyledon-stage embryos (Fig. 2K, L). As a control, no GUS activity appeared in the proembryo of wild-type plants (Fig. 2D).

To validate the distribution of free IAA in proembryos, IAA immunoenzyme localization was used with an anti-IAA antibody. The results showed an even distribution of free IAA in the zygote, the 2-celled stage, and the early proembryo in tobacco (Fig. 2M–O), which was similar to that of the GUS activity assay. As a control, no signal was detected in the embryo when incubated with PBS instead of the primary antibody (Fig. 2P).

In addition, auxin-activated *DR5::GUS* expression was also detected in ovules so that the accumulation of free IAA could be traced in these tissues (see Supplementary Fig. 1 at *JXB* online). It was shown that the GUS signal was very weak in the ovules at the zygote, the 2-celled, and the 8-celled embryo stages (see Supplementary Fig. S1A–C at *JXB* online), while it was strong in the ovules at the early globular to transitional stage embryos (see Supplementary Fig. 1E–H at *JXB* online). Then the GUS staining became weak in ovules of differentiated embryo stages (see Supplementary Fig. S1I–L at *JXB* online).

Effects of exogenous IAA and TIBA on zygote and proembryo development in ovule culture

When 3 DAP ovules were cultured for 4 d, the zygotes inside the ovules developed into proembryos with a different shape (Table 1). Proembryo development was obviously promoted in low concentrations of IAA (0.1 μM), and the frequency of more than 16-celled proembryos increased to 56.2%, which was higher than that in untreated controls (15.07%). Moreover, zygote division and proembryo development were affected to some extent by the treatment with TIBA, an auxin transport inhibitor. When the TIBA concentration was 30 μM, the frequency of proembryos with more than 16 cells decreased to 4.77%, but that of abnormal and dead proembryos increased to 5.06% and 9.13%, respectively. Most of the ovules were dead after treatment with 50 μM TIBA (data not shown).

To investigate the effect of IAA on proembryo differentiation, ovules at the early globular embryo stage (5 DAP) were cultivated in medium supplemented with IAA or TIBA. After 5 d and 10 d of culture, embryos inside the ovules developed into four types: normal undifferentiated and differentiated, and abnormal undifferentiated and differentiated. In IAA-treated ovules, the types of embryo development were similar to the control, while TIBA caused both aberrations and a delay in embryo differentiation (Table 2). The effects of TIBA on proembryo development also appeared in a concentration-dependent manner. Treatment with 50 μM TIBA caused the death of most of the ovules after 10 d of culture (data not shown).

When ovules were transferred into germination medium, embryo germination frequency in 2 μM IAA-treated ovules

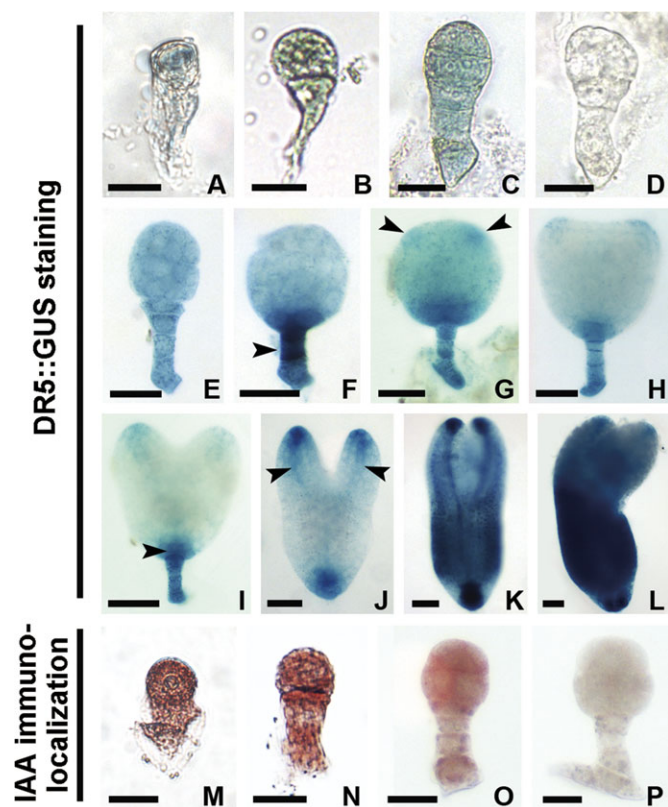


Fig. 2. Localization of IAA in tobacco zygotes and proembryos. (A–C, E–L) Auxin-dependent *DR5::GUS* expression in zygote, 2-celled, 8-celled, early globular, middle globular, late globular, transition-stage, heart-shaped, early torpedo-shaped, late torpedo-shaped, and mature proembryos, respectively. (M–O) Immunoenzyme localization of IAA in the wild-type zygote, 2-celled, and early globular proembryos, respectively. (D, P) The control embryos in wide-type plants with GUS staining (D) or without the primary antibody (P), respectively. Arrowheads indicate the suspensor, cotyledon primordium regions, hypophysis cell region, and provascular strands in (F, G, I, J), respectively. GUS staining in blue (A–C, E–L). IAA signal in brown (M–O). (A–D, M–P) Bar=20 μm; (E–H) bar=40 μm; (I–L) bar=60 μm.



was the highest of all the treatments during the 50 d of culture (Table 3; Fig. 3I), and most of the seedlings had two normal symmetrical cotyledons (Fig. 3A). The frequency of germinated seedlings with normal cotyledons decreased, while those with abnormal cotyledons increased in 10 μM and 30 μM TIBA treatments (Table 3) and was lowest with 30 μM TIBA (Fig. 3I). No seedling germination was observed in the 50 μM TIBA treatment. Furthermore, the

Table 1. Effects of IAA and TIBA on tobacco zygote development in the culture of 3 DAP ovules

Treatment	No. of isolated embryos	Frequency of developed embryos (%) ^a					
		Normal				Abnormal	Dead
		2 to 4-celled	5 to 8-celled	9 to 16-celled	over 16-celled		
–	309	8.85±3.00	22.27±1.79	52.03±7.89	15.07±3.75	1.21±0.28	0.57±1.09
0.1 μM IAA	530	0.37±0.64*	5.07±4.40**	36.83±4.88	56.20±5.02*	1.53±0.14	0
10 μM TIBA	389	11.02±2.87	27.11±4.31	46.10±12.18	12.36±1.15	3.41±0.35	0
30 μM TIBA	290	14.36±3.49	17.09±2.60	49.59±2.74	4.77±0.42*	5.06±7.59*	9.13±4.61**

^a The results are shown with standard errors. The best promotion effect in the IAA-treated group was at any the concentration of 0.1 μM when supplemented with 0.1, 0.3, 0.5 and 1 μM IAA (data not shown). * 0.01 < P < 0.05 indicates a significant difference compared with the untreated group; ** P < 0.01 indicates extremely significant difference compared with the untreated group.

Table 2. Effects of IAA and TIBA on tobacco embryo development in the culture of 5 DAP ovules

Treatment	No. of isolated embryos	Frequency of developed embryos (%) ^a						
		Normal				Abnormal		
		Undifferentiated		Differentiated				
5 d	—	630	52.48±7.79	26.86±6.81	16.16±3.34			3.38±1.29
	2 μM IAA	665	45.62±8.57	28.02±5.93	20.73±3.65	5.00±1.82	0.52±0.36	0.11±0.10
	10 μM TIBA	693	53.04±10.41	26.15±9.96	15.67±8.43	2.64±0.98	1.21±0.75	1.29±0.84
	30 μM TIBA	588	74.90±14.33	10.33±4.54**	8.08±6.11	0.73±0.84**	4.02±1.81*	1.94±0.89
	50 μM TIBA	133	85.62±12.29**	5.08±1.27**	0.56±0.14**	0**	6.11±0.76**	2.63±0.48*
10 d	—	474	1.96±1.21	6.40±2.25	18.20±3.33	69.53±8.68	1.50±0.79	2.41±0.53
	2 μM IAA	648	1.40±1.19	3.14±1.96	7.88±2.62*	83.28±8.07	1.36±1.12	2.94±1.76
	10 μM TIBA	520	4.67±1.72	5.36±1.30	12.79±4.92	63.42±16.13	3.36±1.77	10.40±2.75**
	30 μM TIBA	463	46.71±4.90*	13.81±1.98*	9.36±3.54*	9.01±3.73**	9.95±2.81*	13.36±7.42*

^a *, ** The indications are the same as shown in Table 1. The best promotion effect in the IAA treated group was at a concentration of 2 μM when supplemented with 0.5, 1, 2, and 4 μM IAA (data not shown).

Table 3. Effects of IAA and TIBA on the germination of tobacco cultured ovules

Treatment	Frequency of germination (%) ^a						
	Total	Normal	Abnormal cotyledons				Multiple
			None	Cup-shape	Single	Two asymmetry	
–	49.67±6.10	44.77±6.61	0.83±0.27	0.71±0.53	1.20±1.14	2.16±1.85	0
2 μM IAA	58.34±5.35	50.45±9.40	1.55±0.71	1.05±0.97	2.43±1.01	2.86±1.65	0
10 μM TIBA	49.90±7.91	9.24±1.86**	3.19±1.63	3.11±2.84	4.03±2.49	26.66±8.83**	3.67±8.84*
30 μM TIBA	31.54±11.92	5.73±4.74**	4.94±2.94	4.59±3.58	4.69±2.68	8.77±5.17	2.82±2.18

^a *, ** The indications are the same as shown in Table 1. The number of cultured ovules was about 250–350, and the germination frequency was analysed after the culture for 50 d.

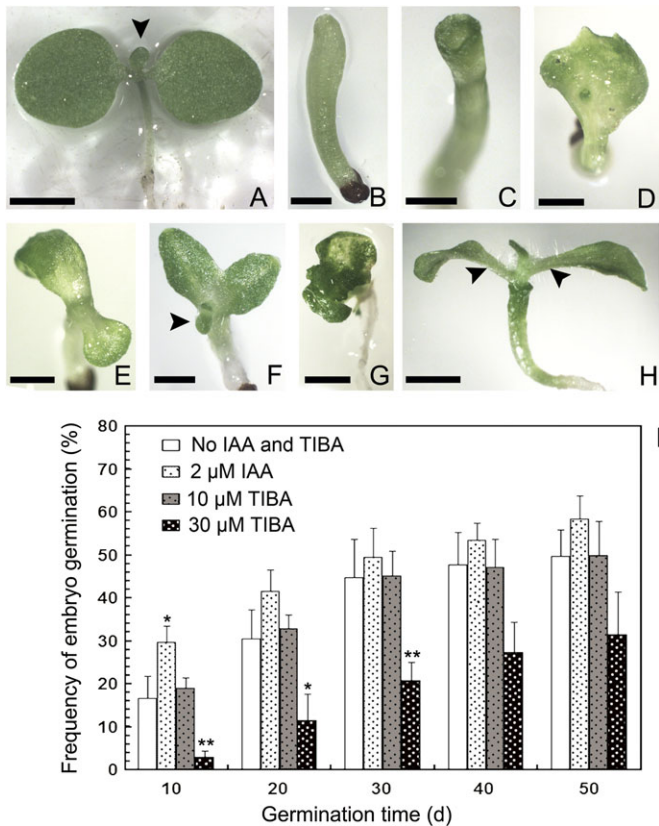


Fig. 3. Embryo germination pattern in tobacco starts from the culture of 5 DAP ovules. (A) A seedling with two symmetrical cotyledons and normal leaf primordia. (B–G) Abnormal seedlings germinated from the ovules treated with TIBA. (B) An abnormal seedling without cotyledons. (C–G) Abnormal seedlings with a cup-shaped cotyledon (C), single cotyledon (D), two asymmetric cotyledons (E, F), and multiple cotyledons (G). (H) A seedling with a cup-shaped cotyledon and normal leaves. The seedling was not transplanted to the normal medium until the embryo germinated in TIBA-treated medium. Arrowheads indicate leaf primordia or leaves in (A, F, H). (I) Effects of IAA and TIBA on the germination frequency of cultured embryos, showing average and the standard error (s.e.) * 0.01 < *P* < 0.05 indicates a significant difference; ** *P* < 0.01 indicates extremely significant difference. Bar=2 mm.

cotyledon phenotype in TIBA-treated seedlings showed various abnormalities, including the lack of cotyledons, only one cotyledon, two asymmetrical cotyledons, and multiple cotyledons (Fig. 3B–G). However, most of the seedlings formed normal leaves after being transplanted into the medium without TIBA (Fig. 3H), which suggests that the effect of TIBA could be reversed when its concentration is lower than 50 μM.

Effect of TIBA on IAA distribution in cultured embryos

In the presence of TIBA, the distribution of free IAA in the cultured embryos was completely disturbed compared with the embryos *in vivo*. In the cultured 3 DAP ovules, GUS expression appeared differently in the abnormal early-

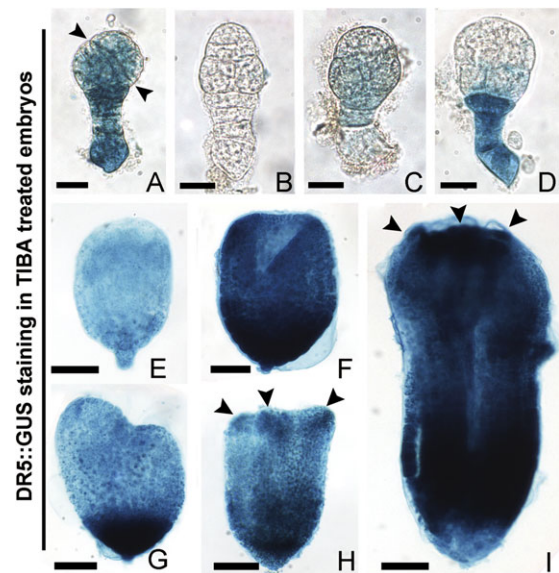


Fig. 4. Auxin-dependent *DR5::GUS* expression in transformed embryos treated with TIBA in tobacco. (A–D) Abnormal early globular embryos from 3 DAP ovules after culture. (A, B) Abnormal globular embryos with asymmetrical division of EP and no apical–basal polarity, respectively. (C) An early globular embryo with faint GUS staining. (D) An abnormal embryo with deep GUS staining in the suspensor. (E) An abnormal undifferentiated embryo from the culture of 5 DAP ovules. (F–I) Abnormal differentiated embryos from the culture of 5 DAP ovules. (F) A cup-shaped embryo. (G–I) Abnormal differentiated embryos with two asymmetrical cotyledon primordia, three cotyledon primordia, and multiple cotyledons, respectively. Arrowheads indicate the division plane of EP cells in (A), cotyledon primordia in (H, I). (A–D) Bar=20 μm; (E) bar=40 μm; (F–I) bar=60 μm.

globular-stage embryos which asymmetrically divided in the EP or lost apical–basal polarity (Fig. 4A–D). In 5 DAP ovules, the GUS signal decreased in the abnormal undifferentiated embryos (Fig. 4E), while it appeared intensely in the basal area and the cotyledon primordia of the abnormal differentiated embryos (Fig. 4F–I). However, when cultured without or with IAA, the normal developed embryos showed a similar GUS signal distribution as *in vivo* (data not shown).

Distribution of ABP1 and PM H⁺-ATPase in isolated zygotes and proembryos

The effect and specificity of the polyclonal antibodies, anti-ABP1 and anti-PM H⁺-ATPase, were examined by Western blot. The proteins from 3–15 DAP ovules were extracted, separated by SDS-PAGE, electroblotted on nitrocellulose membranes, and respectively immunoblotted with the two antibodies. The results showed that the endogenous ABP1 and PM H⁺-ATPase detected were about 25 kDa (Fig. 5A) and 94 kDa (Fig. 5B), respectively.

To investigate whether ABP1 and PM H⁺-ATPase are involved in tobacco zygote and embryo development, their

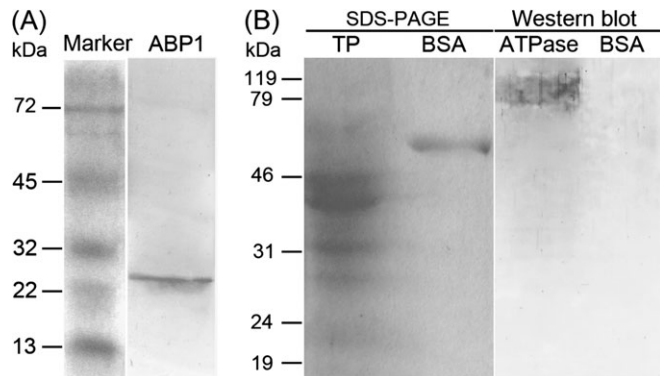


Fig. 5. Western blot of ABP1 and PM H⁺-ATPase in tobacco ovules. (A) ABP1 recognized by polyclonal anti-maize ABP1 antibody. (B) PM H⁺-ATPase recognized by polyclonal antibody which comes from *Nicotiana plumbaginifolia*. In order to exclude the possible interference of BSA, which is part of the antibody dilution buffer and could make a molecular weight marker, the whole NC membrane (transferred with the SDS-PAGE) was hybridized with the antibody of PM H⁺-ATPase. TP, total protein; BSA, bovine serum albumin; ATPase, plasma membrane H⁺-ATPase.

distribution pattern was observed and analysed by immunofluorescence.

The results showed that the ABP1 fluorescent signal was distributed evenly in fertilized egg cells (zygote) with a big nucleus (Fig. 6A–a2). When the zygote elongated, an additional signal appeared in the cell wall of the micropylar region (Fig. 6B–b2). In the 2-celled proembryo, the signal appeared strongly in the nucleus (Fig. 6C–c2), but then diffused to the whole cytoplasm in the 3-celled and the early globular embryo (Fig. 6D–e2). However, in the late globular stage and differentiated embryos, this signal displayed a polar distribution, and was especially located in the junction of the EP and suspensor, the apex of the EP or the cotyledons (Fig. 6F–h). To validate the localization of ABP1 in embryos, cryosection and immunoenzyme techniques were also used, and the results showed that ABP1 was strongly located in the torpedo-shaped embryos (Fig. 6I). In the control, no fluorescence (data not shown) or immune-colour (Fig. 6J) was observed in the embryos.

The distribution of the PM H⁺-ATPase was quite different from ABP1 in the zygote and early proembryos. In the globular and elongated zygote, as well as the 2-celled proembryo, the PM H⁺-ATPase fluorescence signal was strongly located in the whole cell but was weak in the nucleus (Fig. 7A–c2), and had begun to concentrate in the cell junction regions of the early globular proembryo (Fig. 8D–e). However, the PM H⁺-ATPase displayed similar polar distribution patterns as ABP1 in the late globular and differentiated embryos (Fig. 7F–h), and its fluorescence signal was concentrated in the apex of EP and the suspensor cells. By using the cryosection and immunoenzyme techniques, a similar pattern of the PM H⁺-ATPase signal was also observed in the torpedo-shaped embryos (Fig. 7I). In the control, no immune-colour was observed (Fig. 7J).

Effects of TIBA on ABP1 and PM H⁺-ATPase distribution in cultured embryos

The distribution of ABP1 and PM H⁺-ATPase in isolated embryos from TIBA-treated ovules was also detected. The result showed that ABP1 distribution in the embryos was disturbed as compared with the normally developed embryos *in vivo*. In the culture of 3 DAP ovules, the abnormal embryos which lost apical–basal polarity and divided asymmetrically displayed irregular ABP1 distribution (Fig. 8A–b2) with a slightly dispersed PM H⁺-ATPase signal (Fig. 8F–g2). In the culture of 5 DAP ovules, the undifferentiated and differentiated abnormal embryos failed to display the polar location of ABP1 (Fig. 8C–e) and PM H⁺-ATPase (Fig. 8H–j). However, by comparison with the expression patterns *in vivo*, there were similar fluorescence signals of ABP1 and PM H⁺-ATPase in cultured embryos with (see Supplementary Fig. S2 at *JXB* online) or without IAA treatment (data not shown).

Immunogold localization of IAA, ABP1, and PM H⁺-ATPase in early globular embryo cells *in vivo*

By using immunogold and TEM techniques, the distribution of IAA, ABP1, and PM H⁺-ATPase was investigated further in early globular embryo cells (Fig. 9). The results showed that IAA gold particles were distributed most abundantly in the cytoplasm (Fig. 9B), and partly in the nucleus (Fig. 9C), PM, and the plastids of embryo cells (data not shown). ABP1 immunogold granules were mainly distributed in the PM and the cytoplasm near the PM (Fig. 9E), and partly in the endoplasmic reticulum (Fig. 9F) and nucleus (data not shown). However, most of the PM H⁺-ATPase gold particles appeared in the PM of embryo cells (Fig. 9G). The control sections without the primary antibodies showed no gold particles (Fig. 9D, H).

Discussion

Roles of IAA in zygote and early embryo development

Embryogenesis originates from the fertilized egg cell (the zygote). Maintenance of the normal auxin level is essential for embryogenesis, for disruption of the auxin concentration or transportation affects the formation of the apical–basal axis in the embryo (Weijers *et al.*, 2005; Cheng *et al.*, 2007). However, beside the studies of IAA distribution in *Arabidopsis* embryos (from the 2-celled to the torpedo-shaped embryos) and in wheat embryos (from the globular to bilaterally symmetrical embryos) (Fischer-Iglesias *et al.*, 2001; Friml *et al.*, 2003; Rober-Kleber *et al.*, 2003), there have been relatively few research reports regarding the change in auxin level and its role in early embryo development of other flowering-plants. In the present study, the well-established tobacco zygote and embryo isolation method, GUS staining, and the immunolocalization technique are used to observe IAA distribution in the tobacco zygote and in the different stages of the embryo which are

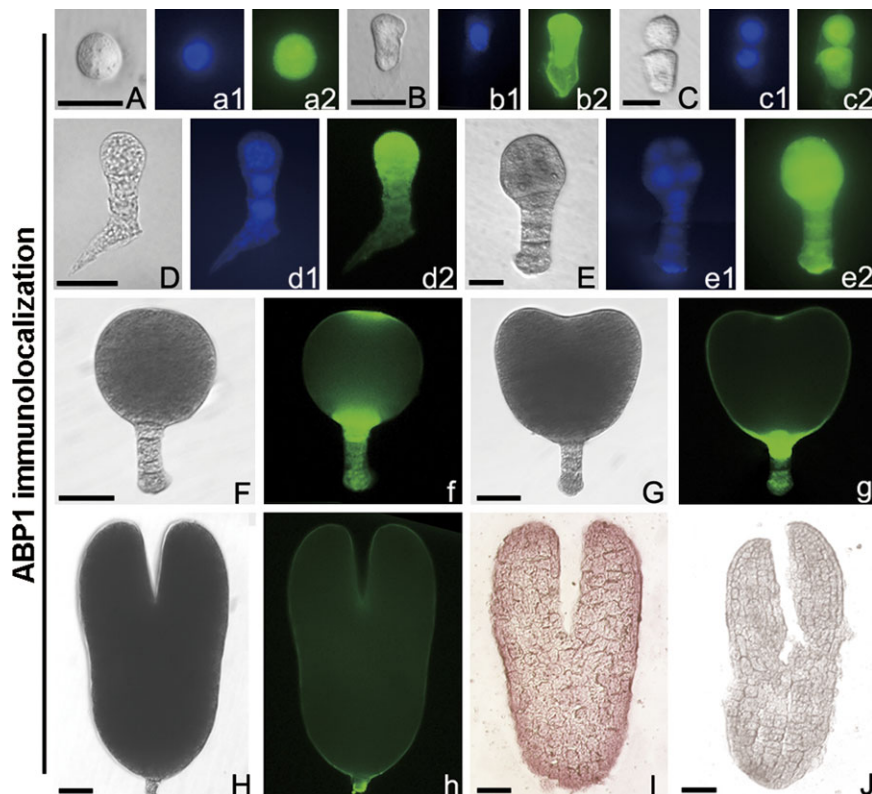


Fig. 6. Immunolocalization of ABP1 in tobacco zygotes and embryos *in vivo*. (A–H) Bright-field images of a globular zygote (A), an elongated zygote (B), a 2-celled embryo (C), a 3-celled embryo (D), an early globular embryo (E), a late globular embryo (F), a heart-shaped embryo (G), and a torpedo-shaped embryo (H). (a1–e1) The corresponding DAPI nuclear counterstain. (a2–e2, f–h) The corresponding ABP1 immunofluorescence images. (I, J) Immunoenzyme labelling of ABP1 and its control images in torpedo-shaped embryos, respectively. (A–E, a1–e1, a2–e2) Bar=20 μm ; (F–J, f–h) bar=40 μm .

deep inside the maternal tissues (as summarized in Fig. 10A). It is reported for the first time that auxin is localized in the the zygote of higher plants. To date, the localization of auxin in the zygote has only been detected in a lower plant, *Fucus distichus* (Basu *et al.*, 2002).

Our results showed a different distribution pattern of IAA in the early embryogenesis of tobacco as compared with *Arabidopsis*. From the zygote to the early globular proembryo in tobacco, the IAA signal was weak and its distribution was even (Figs 2A–C, 10A), while in *Arabidopsis*, it was localized to the poles in the apical cell and the embryo proper of early-stage embryos (Friml *et al.*, 2003). The polar distribution of IAA, together with the mutants and the expression analysis of the auxin efflux genes in *Arabidopsis*, showed the importance of auxin in establishing the apical–basal axis of the embryo (Hamann *et al.*, 1999, 2002; Friml *et al.*, 2003; Weijers *et al.*, 2005). As no there was no detectable polar localization of IAA in the tobacco zygote and early embryos, it is not clear whether free IAA participates in axis establishment. However, by using *in vitro* culture experiments, this assumption was verified. The treatment of zygote-staged ovules with the IAA transport inhibitor TIBA led to the delay of zygote and embryo division and the morphological aberration of embryos (Table 1). Furthermore, IAA distribution was disrupted in TIBA-treated abnormal embryos (Fig. 4A–D). Thus, the

normal distribution of IAA in the zygote and early proembryo is required for the directional differentiation of proembryo cells. The immunogold localization results show that abundant IAA exists in the cytoplasm of the early globular proembryo (Fig. 9C), and this suggests the presence of active auxin signal transduction.

But, why is the distribution of IAA different in early embryos of tobacco and *Arabidopsis*? It is presumed that one reason is the discrepancy in cell division pattern and arrangement during early embryo development. Although both tobacco and *Arabidopsis* are model dicotyledons, their cell division patterns and arrangement orders are quite different in the early embryo stage. In *Arabidopsis*, the apical cell of the 2-celled proembryo first undergoes two longitudinal and then a transverse division to form an octant-stage embryo, while the basal cell undergoes more than one division before the second division of the apical cell and there is a multicellular (over 4-celled) suspensor in the octant-stage embryo (Berleth and Chatfield, 2002; Friml *et al.*, 2003). In tobacco, the apical cell of the 2-celled proembryo first undergoes a transverse and then two longitudinal divisions to form an octant-stage embryo, while the first division of the basal cell follows closely after the first division of the apical cell and there is a suspensor with four cells in the octant-stage embryo (data not shown). Therefore, this differentiation indicates that the different

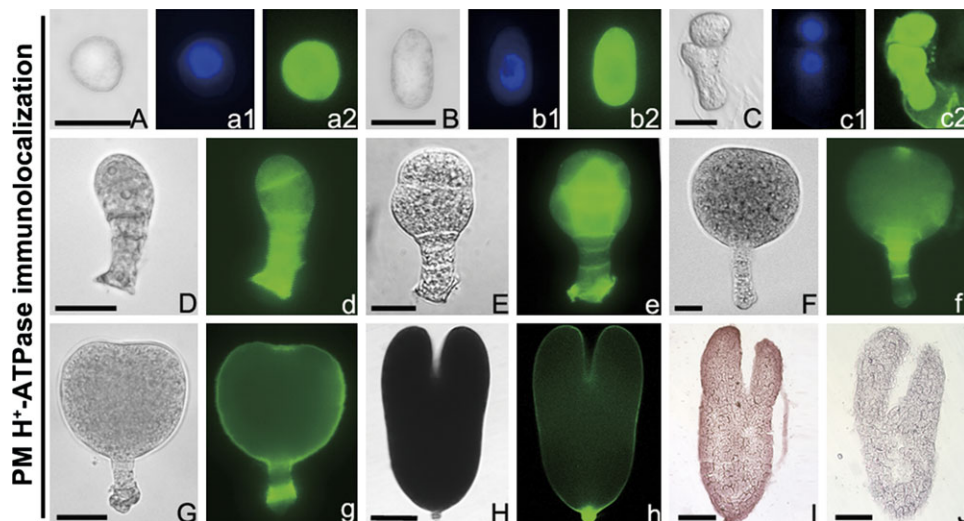


Fig. 7. Immunolocalization of PM H⁺-ATPase in tobacco zygotes and embryos *in vivo*, (A–H) Bright-field images of a globular zygote (A), an elongated zygote (B), a 2-celled embryo (C), a 5-celled embryo (D), an early globular embryo (E), a late globular embryo (F), an early heart-shaped embryo (G), and a torpedo-shaped embryo (H). (a1–c1) The corresponding DAPI nuclear counterstain. (a2–c2, d–h) The corresponding PM H⁺-ATPase immunofluorescence images. (I, J) Immunoenzyme localization of PM H⁺-ATPase and its control in torpedo-shaped embryo, respectively. (A–F) Bar=20 μm; (G–J) bar=60 μm.

molecular mechanisms of auxin response, which control the cell division pattern and arrangement order, possible exist in early embryogenesis of tobacco and *Arabidopsis*.

It is presumed that free auxin is transported from the maternal tissue to the zygote and initiates the formation of the embryo polar axis (Friml *et al.*, 2003), but there was still a lack of experimental evidence. In this study, it was found that exogenous IAA at a low concentration significantly promoted zygote division and early embryo development in *in vitro* ovule culture (Table 1). However, *in vivo*, the level of IAA was very low in tobacco ovules at the zygote and the 2-celled proembryo stages (Fig. 1C), and the *DR5::GUS* expression of ovules was also weak from the zygote to the early embryo stages (see Supplementary Fig. 1A–C at *JXB* online). It suggests that the IAA level was low in the ovule, the zygote, and the early stages of embryos. Perhaps there was an auxin transport route from the maternal tissue into the ovule and zygote during this process in tobacco. In addition, it was found that abundant IAA is distributed in the placenta and vascular tissues of 4–5 DAP ovaries (data not shown) when the zygote developed into the 2-celled to 8-celled proembryos, which suggests that there is polar transportation of IAA from the vascular bundle and placenta of the ovary to the ovule and zygote in early embryogenesis.

Roles of IAA in embryo differentiation and maturation

After a zygote develops into a globular embryo, the cells of the EP will undergo organ primordium differentiation instead of continuous periclinal division. Localized cell divisions lead to the emergence of various specialized regions: along the apical–basal axis will form the shoot apical meristem, cotyledons, hypocotyls, and the root apical meristem. The dynamic expression pattern of *DR5::GUS* in

Arabidopsis embryos is closely related to the function of auxin for establishing and maintaining the apical meristem and cotyledons (Hamann *et al.*, 2002; Friml *et al.*, 2003; Aida *et al.*, 2004; Furutani *et al.*, 2004; Hardtke *et al.*, 2004; Bliou *et al.*, 2005; Jenik and Barton, 2005). In tobacco, a temporal and spatial *DR5::GUS* expression was also found, which appears to be similar to the auxin distribution in *Arabidopsis* embryos (Figs 2F–L; 10A): from accumulation in the basal area of the EP and suspensor in the middle globular embryo and into the cotyledon tip, provascular strands, and root meristem in the torpedo-shaped embryo. Although there are differences, as in early embryogenesis, the similar distribution pattern during embryo differentiation and maturation in *Arabidopsis* and tobacco implies a similar function of auxin. In cultured tobacco ovules at the globular embryo stage, TIBA treatment not only led to the delay of embryo differentiation, maturation, and germination, but also caused embryo aberration and cotyledon abnormality (Tables 2, 3; Figs 3, 4, 8). Some phenotypes of the abnormal seedlings strongly resembled *pin* mutants in *Arabidopsis*, for example, the cup-shaped and single cotyledon seedlings (Fig. 3C, D) also appeared in the *pin1pin3pin4pin7* and *pin4pin7* mutants, respectively (Friml *et al.*, 2003). Furthermore, the IAA distribution pattern was irregular in abnormal embryos treated with TIBA (Fig. 4E–I). Our results suggest that normal IAA levels and distribution are essential for cotyledon differentiation and embryo maturation in tobacco, which is consistent with the roles of IAA in *Arabidopsis* embryos.

The study on YUCCA flavin monooxygenase, a key enzyme in the auxin synthesis pathway in *Arabidopsis*, suggests that auxin was possibly synthesized in the apical region of embryos and transported into the hypophysis to regulate the division and differentiation of root meristems

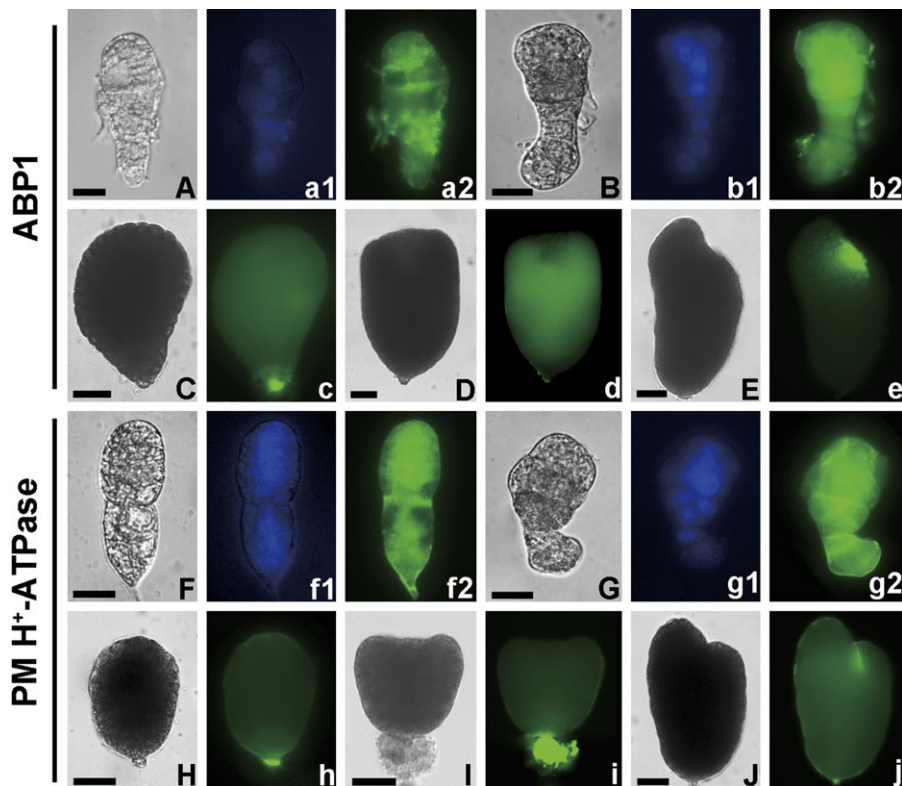


Fig. 8. Immunolocalization of ABP1 and PM H⁺-ATPase in tobacco abnormal embryos treated with TIBA *in vitro*. (A–J) Bright-field images. (A, B, F, G) Abnormal early globular embryos from the culture of 3 DAP ovules have lost the apical–basal polarity (A, F) and asymmetrical division in the embryo proper (B, G). (a1, b1, f1, g1) The corresponding DAPI nuclear counterstain. (a2, b2, c–e) The corresponding ABP1 immunofluorescence images in (A–E). (f2, g2, h–j) The corresponding PM H⁺-ATPase immunofluorescence images in (F–J). (C, H) Abnormal undifferentiated embryos from the culture of 5 DAP ovules. (D, E, I, J) Abnormal differentiated embryos with cup-shaped cotyledon primordia, single cotyledon primordia, three cotyledon primordia, and asymmetric cotyledons from the culture of 5 DAP ovules, respectively. (A, B, F, G) Bar=20 μ m; (C–E, H–J) bar=40 μ m.

during embryo development (Friml *et al.*, 2003; Cheng *et al.*, 2007). Together with embryo differentiation and maturation, the IAA level in the whole tobacco ovule dramatically increased (Fig. 1C), while *DR5::GUS* expression was not very strong at the ovule surface during this period (see Supplementary Fig. S1F–L at *JXB* online), which indicates increased amounts of IAA in the embryo, as if there is active auxin biosynthesis in embryos. Although there is no genetic evidence, the similar distribution pattern of IAA during embryo differentiation and maturation in *Arabidopsis* and tobacco suggests that a similar source of auxin may exist in these two types of plant embryos.

Possible involvement of ABP1 in auxin-dependent embryogenesis

ABP1 has long been considered as an important potential receptor of auxin. Many researchers have demonstrated its receptor function in mediating auxin-dependent cell division and expansion, such as in maize coleoptiles, shoots, and roots (Henderson *et al.*, 1997; Venis *et al.*, 1992; Steffens *et al.*, 2001), tobacco leaves and BY2 cells (Chen *et al.*, 2001a; David *et al.*, 2007; Braun *et al.*, 2008), and *E. ulmoides* stems (Hou *et al.*, 2006). It was shown that ABP1 present in the

shoot meristem and the epidermal cells of the scutellum in maize immature embryos (Bronsema *et al.*, 1998). However, the lethality of the early globular-staged embryo in the mutant of *ABP1* in *Arabidopsis* (Chen *et al.*, 2001b) prevents any further study of this gene in embryo development.

In this paper, the first information for characterizing the elaborate temporal and spatial distribution of ABP1 in tobacco embryo development by using immunolocalization techniques is provided. Our results showed that the ABP1 signal was intense in the tobacco zygote and embryo *in vivo* (Fig. 6, and summarized in Fig. 10B), distributed evenly in the zygote and polar in the apical region of the EP, and in the the cells between the EP and the suspensor in the heart-embryo and the torpedo-embryo. The distribution pattern of ABP1 which varied with the different developmental stages implies that this protein participates in embryo development and differentiation. As a potential receptor of auxin, the role of ABP1 in embryogenesis is possibly related to the auxin response. To validate this hypothesis, the expression of ABP1 was investigated in tobacco embryos dissected from the cultured ovules. The result showed that the addition of TIBA perturbed the normal distribution of ABP1 in cultured embryos (Fig. 8a2, b2, c–e), which implied that ABP1 may participate in auxin-dependent embryo development.

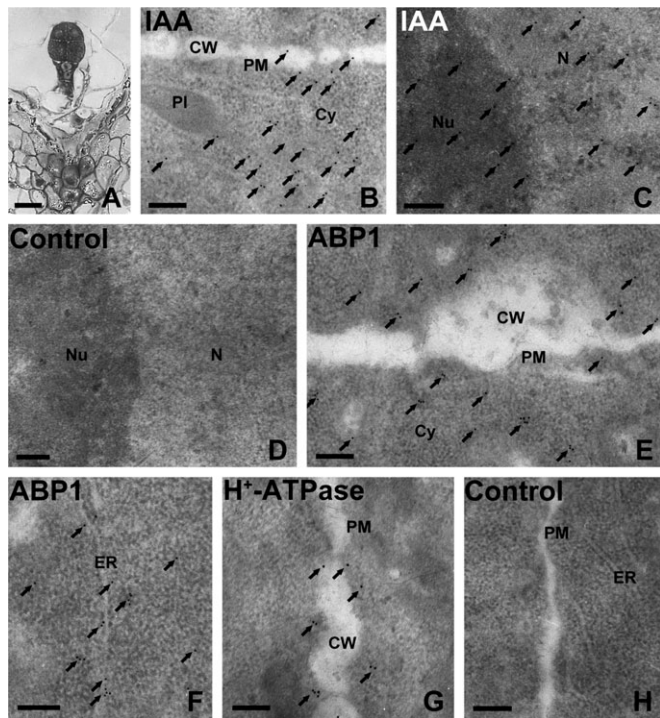


Fig. 9. Immunogold localization of IAA, ABP1, and PM H⁺-ATPase in the early globular embryo (5 DAP) of tobacco. (A) Semi-thin section of an early globular embryo. (B–H) Ultrathin sections of the early globular embryo, showing IAA, ABP1, and PM H⁺-ATPase immunogold granules, respectively. (B) Numerous IAA gold particles appeared in the cytoplasm near the cell wall, and a few were distributed in the plasma membrane (PM) and cell wall of the embryo. (C) Many IAA gold particles accumulated in the nucleus. (D) A control section without the primary IAA antibody, and the secondary antibody was a goat anti-rat IgG antibody. The image showed no gold particles. (E, F) ABP1 gold particles mainly distributed in the PM and cytoplasm near the cell wall (E) and in the ER (F). (G) Nearly all PM H⁺-ATPase gold particles appeared in the PM. Arrows indicate the gold particles. (H) A control section without the primary antibodies of ABP1 or PM H⁺-ATPase, while the secondary antibody was goat anti-rabbit IgG antibody. The image showed no gold particles. (A) Bar=25 µm; (B) bar=5 µm; (C–E) bar=0.2 µm; Cy, cytoplasm; CW, cell wall; ER, endoplasmic reticulum; N, nucleus; Nu, nucleolus; PI, plastid; PM, plasma membrane.

Cell elongation and division are two essential auxin-mediated responses that are related to ABP1 (Jones *et al.*, 1998; Chen *et al.*, 2001a, b; David *et al.*, 2007; Braun *et al.*, 2008). Previous work indicated that extracellular ABP1 has the function as a physiological receptor for cell expansion. ABP1 is usually stored in the endoplasmic reticulum and is secreted into the plasma membrane (PM) or the cell exterior via Golgi bodies (Venis *et al.*, 1992; Bronsema *et al.*, 1998; Shimomura *et al.*, 1999; Christian *et al.*, 2006). By conditional expression of a single-chain fragment variable (scFv), which was derived from an antibody fragment directed against ABP1, endogenous ABP1 was inactivated and this led to the blocking of the cell cycle. Further

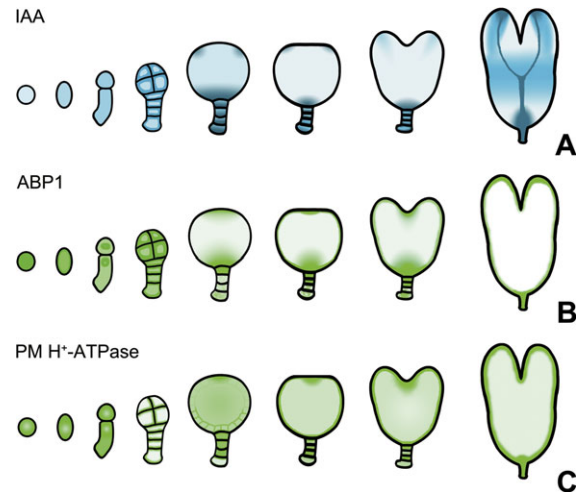


Fig. 10. A schematic diagram showed the gradual changes of IAA, ABP1, and PM H⁺-ATPase levels during tobacco zygote and embryo development. The colour marks the expression of *DR5::GUS* in blue (A), and ABP1 (B) and PM H⁺-ATPase (C) in green. The degree of colour represents the signal strength.

research provided evidence that ABP1 played a critical role in auxin-mediated cell division by acting on the G₁/S and G₂/M checkpoints (David *et al.*, 2007). In this study, numerous ABP1 gold particles were observed in the PM at the junction between the early globular embryo cells which is the possible functional site in auxin-mediated cell expansion (Fig. 9). Also, the presence of ABP1 in the cytoplasm and nucleus which overlapped with IAA distribution could be explained by their probable roles in regulating embryo cell division. Although no direct evidence provides the function of ABP1 in early embryogenesis, our results suggest that ABP1 might play roles in cell elongation and division of the zygote and embryo. Furthermore, the change in auxin distribution in the zygote and embryo is probably function related to ABP1 (Fig. 10A, B). In *Arabidopsis*, the embryo development of the *ABP1* mutant ceased in the early-globular-embryo stage, and was unable to undergo any further cell division, growth, and differentiation (Chen *et al.*, 2001b). Our research on the dynamic distribution of ABP1 during embryo differentiation indicates the possible function of ABP1 in regulating the division of the shoot and root apical meristem. The distribution of ABP1 and IAA is different in the apical region of the EP, but similar in the basal region of the EP (Fig. 10A, B); this suggests that ABP1 might take part in different auxin response pathways in these two areas.

Possible involvement of PM H⁺-ATPase in auxin-dependent embryogenesis

Although many genes have been identified as members of an auxin signal transduction network in embryogenesis, the molecular mechanisms of how auxin acts on the establishment of the apical–basal axis and on the formation of embryonic organs is not clear. The PM H⁺-ATPase is

suggested to be a downstream target of the auxin signalling pathway (Harper *et al.*, 1994; Frías *et al.*, 1996). It has been reported that the PM H⁺-ATPase may be involved in auxin-mediated embryo cell elongation in the typical monocotyledon wheat, for it was strongly localized in the epidermal cells of the scutellum at the bilaterally symmetrical stage and its expression and activity was regulated by auxin (Rober-Kleber *et al.*, 2003). However, until now, no report has shown the involvement of the PM H⁺-ATPase in the early embryogenesis of dicotyledonous plants. Due to the lack of information about the role of PM H⁺-ATPase in embryogenesis, the changes of PM H⁺-ATPase were investigated during zygote and embryo development in tobacco (Figs 7, 10C) by using the immunolocalization technique. This technique was previously used in the study of PM H⁺-ATPase distribution in *Torenia fournieri* pollen tubes (Wu *et al.*, 2008), *Nicotian plumbaginifolia* pollen tubes (Lefebvre *et al.*, 2005), *Triticum aestivum* embryos (Rober-Kleber *et al.*, 2003), and *Lilium longiflorum* pollen grains and pollen tubes (Obermeyer *et al.*, 1992). In the present study, the dynamic distribution pattern of the PM H⁺-ATPase shows that it is developmentally regulated. Moreover, the disordered distribution of the PM H⁺-ATPase was observed in the abnormal embryos induced by TIBA (Fig. 8f2, g2, h–j), which indicated that the expression pattern of the PM H⁺-ATPase is probably regulated by IAA during embryo development.

Interestingly, the distribution of PM H⁺-ATPase was similar to that of ABP1 during tobacco embryo differentiation and maturation as summarized in Fig. 10B, C. ABP1 is considered as a component that connects the auxin signal with the PM H⁺-ATPase (Macdonald, 1997; Christian *et al.*, 2006). Thus, the overlapping in the specific regions, including the shoot and root apical meristem of the embryos, revealed a function correlation between the PM H⁺-ATPase and ABP1. Based on a classical auxin-induced cell elongation model, ‘acid-growth theory’, the exposure of responsive cells to auxin leads to the excretion of H⁺ out of the PM, presumably either by increasing the amount of the PM H⁺-ATPase or by combination with ABP1, stimulating the activity of the PM H⁺-ATPase in the PM, and then the decreased pH value causes the apoplastic acidification and cell wall loosening, which results in cell elongation (Christian *et al.*, 2006). In this study, the subcellular localization in the early globular embryos displays the presence of the PM H⁺-ATPase in the PM at the junctions between embryo cells, where ABP1 is also abundant (Fig. 9). The same localization of the PM H⁺-ATPase and ABP1 in the PM is in accordance with the ‘acid-growth theory’. Their expression in the apical and basal areas of the EP during embryo differentiation is likely to contribute to the formation of the shoot and root apical meristem in tobacco.

Embryo development in higher plants is a complex process. Compared with IAA and ABP1 in zygote and early proembryos, the distribution of PM H⁺-ATPase is quite different (Fig. 10). Considering the role of the PM H⁺-ATPase in the control of various cell physiological activities, such as contributing to nutrient uptake in broad bean

embryos (Bouche-Pillon *et al.*, 1994), suggests that the role of the PM H⁺-ATPase in early embryogenesis might be mediated by other factors. However, its function and molecular mechanism during embryo development is far from clear, and needs to be investigated further.

Conclusion

This study shows the level and distribution of free IAA in different developmental stages of tobacco ovules, and the temporal and spatial distribution of IAA, ABP1, and PM H⁺-ATPase in the zygote and embryos. In ovule culture, zygote division, embryo differentiation and maturation, and organ formation were all promoted by suitable concentration of IAA, but suppressed by TIBA, an inhibitor of auxin polar transport. By immunolocalization techniques, it was found that the distribution of IAA, ABP1, and PM H⁺-ATPase were all disturbed in abnormal embryos treated by TIBA. These results indicate that the polar distribution of free IAA may begin from the zygote and change regularly to ensure subsequent embryo formation and differentiation. ABP1 and PM H⁺-ATPase are probably involved in these processes and are correlated to auxin signalling transduction during embryo development.

Supplementary data

Supplementary data can be found at JXB online.

Supplementary Fig. 1. Auxin-dependent *DR5::GUS* expression in transformed tobacco ovules.

Supplementary Fig. 2. Immunolocalization of ABP1 and PM H⁺-ATPase in normal tobacco embryos without treatment *in vitro*.

Acknowledgements

The authors thank Professor Marc Boutry (Unité de Biochimie Physiologique, Institut des Sciences de la Vie, Université Catholique de Louvain-la-Neuve, Belgium) for the generous gift of the anti-PM-H⁺-ATPase antibody, and Professor Richard Napier (Crop Improvement and Biotechnology, Horticulture Research International, UK) for the generous gift of the anti-ABP1 antibody and his suggestions. This work is supported by the Major State Basic Research Program of China (2007CB108704) and the National Natural Science Foundation of China (30821064, 30970277).

References

- Aida M, Beis D, Heidstra R, Willemsen V, Blilou I, Galinha C, Nussaume L, Noh YS, Amasino R, Scheres B. 2004. The *PLETHORA* genes mediate patterning of the *Arabidopsis* root stem cell niche. *Cell* **119**, 109–120.

- Basu S, Sun HG, Brian L, Quatrano RL, Muday GK.** 2002. Early embryo development in *Fucus distichus* is auxin sensitive. *Plant Physiology* **130**, 292–302.
- Braun N, Wyrzykowska J, Muller P, David K, Couch D, Perrot-Rechenmann C, Fleming AJ.** 2008. Conditional repression of AUXIN BINDING PROTEIN1 reveals that it coordinates cell division and cell expansion during postembryonic shoot development in *Arabidopsis* and tobacco. *The Plant Cell* **20**, 2746–2762.
- Berleth T, Chatfield S.** 2002. Embryogenesis: pattern formation from a single cell. In: Somerville CR, Meyerowitz EM, eds. *The Arabidopsis book*, Vol.7. The American Society of Plant Biologists, 1–88.
- Bliilou I, Xu J, Wildwater M, Willemsen V, Paponov I, Friml J, Heidstra R, Aida M, Palme K, Scheres B.** 2005. The PIN auxin efflux facilitator network controls growth and patterning in *Arabidopsis* roots. *Nature* **433**, 39–44.
- Bronsema FBF, van Oostveen WJF, van Lammeren AAM.** 1998. Immunocytochemical localisation of auxin-binding proteins in coleoptiles and embryos of *Zea mays* L. *Protoplasma* **202**, 65–75.
- Bouche-Pillon S, Fleurat-Lessard P, Serrano R, Bonnemain JL.** 1994. Asymmetric distribution of the plasma-membrane H⁺-ATPase in embryos of *Vicia faba* L. with special reference to transfer cells. *Planta* **193**, 392–397.
- Chen D, Zhao J.** 2008. Free IAA in stigmas and styles during pollen germination and pollen tube growth of *Nicotiana tabacum*. *Physiologia Plantarum* **134**, 202–215.
- Chen JG, Shimomura S, Sitbon F, Sandberg G, Jones AM.** 2001a. The role of auxin-binding protein 1 in the expansion of tobacco leaf cells. *The Plant Journal* **28**, 607–617.
- Chen JG, Ullah H, Young JC, Sussman MR, Jones AM.** 2001b. ABP1 is required for organized cell elongation and division in *Arabidopsis* embryogenesis. *Gene and Development* **15**, 902–911.
- Cheng YF, Dai XH, Zhao YD.** 2007. Auxin synthesized by the YUCCA flavin monooxygenases c is essential for embryogenesis and leaf formation in *Arabidopsis*. *The Plant Cell* **20**, 1790–1799.
- Christian M, Steffens B, Schenck D, Burmester S, Böttger M, Lüthen H.** 2006. How does auxin enhance cell elongation? Roles of auxin-binding proteins and potassium channels in growth control. *Plant Biology* **8**, 346–352.
- David KM, Couch D, Braun N, Brown S, Grosclaude J, Perrot-Rechenmann C.** 2007. The auxin-binding protein 1 is essential for the control of cell cycle. *The Plant Journal* **50**, 197–206.
- Ding XH, Cao YL, Huang LL, Zhao J, Xu CG, Li XH, Wang SP.** 2008. Activation of the indole-3-acetic acid-amido synthetase GH3-8 suppresses expansin expression and promotes salicylate- and jasmonate-independent basal immunity in rice. *The Plant Cell* **20**, 228–240.
- Fischer C, Neuhaus G.** 1996. Influence of auxin on the establishment of bilateral symmetry in monocots. *The Plant Journal* **9**, 659–669.
- Fischer C, Speth V, Fleig-Eberenz S, Neuhaus G.** 1997. Induction of zygotic polyembryos in wheat: influence of auxin polar transport. *The Plant Cell* **9**, 1767–1780.
- Fischer-Iglesias C, Sundberg B, Neuhaus G, Jones AM.** 2001. Auxin distribution and transport during embryonic pattern formation in wheat. *The Plant Journal* **26**, 115–129.
- Frias I Caldeira MT, Pérez-Castilleira JR, Navarro-Aviñó Juan P, Culiáez-Maciá FA, Kuppinger O, Stransky H, Pagés M, Hager A, Serrano R.** 1996. A major isoform of the maize plasma membrane H⁺-ATPase: characterization and induction by auxin in coleoptiles. *The Plant Cell* **8**, 1533–1544.
- Friml J, Vieten A, Sauer M, Weijers D, Schwarz H, Hamann T, Offringa R, Jürgens G.** 2003. Efflux-dependent auxin gradients establish the apical–basal axis of *Arabidopsis*. *Nature* **426**, 147–153.
- Furutani M, Vernoux T, Traas J, Kato T, Tasaka M, Aida M.** 2004. PIN-FORMED1 and PINOID regulate boundary formation and cotyledon development in *Arabidopsis* embryogenesis. *Development* **131**, 5021–5030.
- Hadfi K, Speth V, Neuhaus G.** 1998. Auxin-induced developmental patterns in *Brassica juncea* embryos. *Development* **125**, 879–887.
- Hamann T, Mayer U, Jürgens G.** 1999. The auxin-insensitive bodenlos mutation affects primary root formation and apical-basal patterning in the *Arabidopsis* embryo. *Development* **126**, 1387–1395.
- Hamann T, Benková E, Bäurle I, Kientz M, Jürgens G.** 2002. The *Arabidopsis* BODENLOS gene encodes an auxin response protein inhibiting MONOPTEROS-mediated embryo patterning. *Genes and Development* **16**, 1610–1615.
- Hardtke CS, Berleth T.** 1998. The *Arabidopsis* gene MONOPTEROS encodes a transcription factor mediating embryo axis formation and vascular development. *The EMBO Journal* **17**, 1405–1411.
- Hardtke CS, Ckurshumova W, Vidaurre DP, Singh SA, Stamatou G, Tiwari SB, Hagen G, Guilfoyle TJ, Berleth T.** 2004. Overlapping and non-redundant functions of the *Arabidopsis* auxin response factors MONOPTEROS and NONPHOTOTROPIC HYPOCOTYL4. *Development* **131**, 1089–1100.
- Harper JF, Manney L, Sussman MR.** 1994. The plasma membrane H⁺-ATPase gene family in *Arabidopsis*: genomic sequence of AHA10 which is expressed primarily in developing seeds. *Molecular and General Genetics* **244**, 572–587.
- Henderson J, Baully JM, Ashford DA, Oliver SC, Hawes CR, Lazarus CM, Venis MA, Napier RM.** 1997. Retention of maize auxin-binding protein in the endoplasmic reticulum: quantifying escape and the role of auxin. *Planta* **202**, 313–323.
- Hou HW, Zhou YT, Mwange KNK, Li WF, He XQ, Cui KM.** 2006. ABP1 expression regulated by IAA and ABA is associated with the cambium periodicity in *Eucommia ulmoides* Oliv. *Journal of Experimental Botany* **57**, 3857–3867.
- Jenik PD, Barton MK.** 2005. Surge and destroy: the role of auxin in plant embryogenesis. *Development* **132**, 3577–3585.
- Jones AM, Im KH, Savka MA, Wu MJ, De Witt NG, Shillito R, Binns AN.** 1998. Auxin-dependent cell expansion mediated by overexpressed auxin-binding protein 1. *Science* **282**, 1114–1117.
- Kim YS, Min JK, Kim D, Jung J.** 2001. A soluble auxin-binding protein, ABP57. Purification with anti-bovine serum albumin antibody and characterization of its mechanistic role in the auxin effect on plasma membrane H⁺-ATPase. *Journal of Biological Chemistry* **276**, 10730–10736.
- Larsson E, Sitbon F, Ljung K, von Arnold S.** 2008. Inhibited polar auxin transport results in aberrant embryo development in Norway spruce. *New Phytologist* **177**, 356–366.

- Lefebvre B, Arango M, Oufattole M, Crouzet J, Purnelle B, Boutry M.** 2005. Identification of a *Nicotiana plumbaginifolia* plasma membrane H⁺-ATPase gene expressed in the pollen tube. *Plant Molecular Biology* **58**, 775–787.
- Liu CM, Xu Z, Chua NH.** 1993. Auxin polar transport is essential for the establishment of bilateral symmetry during early plant embryogenesis. *The Plant Cell* **5**, 621–630.
- Macdonald H.** 1997. Auxin perception and signal transduction. *Physiologia Plantarum* **100**, 423–430.
- Merlot S, Leonhardt N, Fenzi F, et al.** 2007. Constitutive activation of a plasma membrane H⁺-ATPase prevents abscisic acid-mediated stomatal closure. *The EMBO Journal* **26**, 3216–3226.
- Morsomme P, Dambly S, Maudoux O, Boutry M.** 1998. Single point mutations distributed in 10 soluble and membrane regions of the *Nicotiana plumbaginifolia* plasma membrane PMA2 H⁺-ATPase activate the enzyme and modify the structure of the C-terminal region. *Journal of Biological Chemistry* **273**, 34837–34842.
- Napier RM, Venis MA.** 1992. Epitope mapping reveals conserved regions of an auxin-binding protein. *Biochemical Journal* **24**, 841–845.
- Obermeyer G, Lutzelschwab M, Heumann HG, Weisenseel MH.** 1992. Immunolocalization of H⁺-ATPases in the plasma membrane of pollen grains and pollen tubes of *Lilium longiflorum*. *Protoplasma* **171**, 55–63.
- Qin Y, Zhao J.** 2006. Localization of arabinogalactan proteins in egg cells, zygotes, and two-celled proembryos and effects of β-D-glucosyl Yariv reagent on egg cell fertilization and zygote division in *Nicotiana tabacum* L. *Journal of Experimental Botany* **57**, 2061–2074.
- Ren YJ, Zhao J.** 2009. Functional analysis of the rice metallothionein gene *OsMT2b* promoter in transgenic *Arabidopsis* plants and rice germinated embryos. *Plant Science* **176**, 528–538.
- Ribnicky DM, Cohen JD, Hu WS, Cooke TJ.** 2002. An auxin surge following fertilization in carrots: a mechanism for regulating plant totipotency. *Planta* **214**, 505–509.
- Rober-Kleber N, Albrechtová JTP, Fleig S, Huck N, Michalke W, Wagner E, Speth V, Neuhaus G, Fischer-Iglesias C.** 2003. Plasma membrane H⁺-ATPase is involved in auxin-mediated cell elongation during wheat embryo development. *Plant Physiology* **131**, 1302–1312.
- Shimomura S, Watanabe S, Ichikawa H.** 1999. Characterization of auxin-binding protein 1 from tobacco: content, localization and auxin-binding activity. *Planta* **209**, 118–125.
- Sondergaard TE, Schulz A, Palmgren MG.** 2004. Energization of transport processes in plants. Roles of the plasma membrane H⁺-ATPase. *Plant Physiology* **136**, 2475–2482.
- Steffens B, Feckler C, Palme K, Christian M, Böttger M, Lüthen H.** 2001. The auxin signal for protoplast swelling is perceived by extracellular ABP1. *The Plant Journal* **27**, 591–599.
- Steinmann T, Geldner N, Grebe M, Mangold S, Jackson CL, Paris S, Gälweiler L, Palme K, Jürgens G.** 1999. Coordinated polar localization of auxin efflux carrier PIN1 by GNOM ARF GEF. *Science* **286**, 316–318.
- Tao LZ, Cheung AY, Wu HM.** 2002. Plant Rac-like GTPase are activated by auxin and mediate auxin-responsive gene expression. *The Plant Cell* **14**, 2745–2760.
- Ulmasov T, Murfett J, Hagen G, Guilfoyle TJ.** 1997. Aux/IAA proteins repress expression of reporter genes containing natural and highly active synthetic auxin response elements. *The Plant Cell* **9**, 1963–1971.
- Venis MA, Napier RM, Barbier-Brygoo H, Maurel C, Perrot-Rechenmann C, Guern J.** 1992. Antibodies to a peptide from the maize auxin-binding protein have auxin agonist activity. *Proceedings of the National Academy of Sciences, USA* **89**, 7208–7212.
- Weijers D, Sauer M, Meurette O, Friml J, Ljung K, Sandberg G, Hooykaas P, Offringa R.** 2005. Maintenance of embryonic auxin distribution for apical-basal patterning by PIN-FORMED dependent auxin transport in *Arabidopsis*. *The Plant Cell* **17**, 2517–2526.
- Wu JZ, Lin Y, Zhang XL, Pang DW, Zhao J.** 2008. IAA stimulates pollen tube growth and mediates the modification of its wall composition and structure in *Torenia fournieri*. *Journal of Experimental Botany* **59**, 2529–2543.
- Yamagami M, Haga K, Napier RM, Iino M.** 2004. Two distinct signalling pathways participate in auxin-induced swelling of pea epidermal protoplasts. *Plant Physiology* **134**, 735–747.
- Zhang XL, Ren YJ, Zhao J.** 2008. Roles of extensins in cotyledon primordium formation and shoot apical meristem activity in *Nicotiana tabacum*. *Journal of Experimental Botany* **59**, 4045–4058.